

# Involvement of *de novo* ceramide synthesis in radiocontrast-induced renal tubular cell injury

Y Itoh<sup>1</sup>, T Yano<sup>1</sup>, T Sendo<sup>1</sup>, M Sueyasu<sup>1</sup>, K Hirano<sup>2</sup>, H Kanaide<sup>2</sup> and R Oishi<sup>1</sup>

<sup>1</sup>Department of Pharmacy, Kyushu University Hospital, Higashi-ku, Fukuoka, Japan and <sup>2</sup>Department of Molecular Cardiology, Research Institute of Angiocardiology, Graduate School of Medical Sciences, Kyushu University, Higashi-ku, Fukuoka, Japan

We reported previously that various radiocontrast media cause apoptosis in porcine proximal tubular (LLC-PK<sub>1</sub>) cells, in which reduction in B-cell lymphoma (Bcl)-2 expression and caspase-3 activation are implicated. In the present study, we investigated a role for ceramide in radiocontrast media-induced apoptosis in renal tubular cells. LLC-PK<sub>1</sub> cells were exposed to radiocontrast media for 30 min, followed by incubation for 24 h in normal medium. Cell viability was assessed by 2-(2-methoxy-4-nitrophenyl)-3-(4-nitrophenyl)-5-(2,4-disulfophenyl)-2H-tetrazolium monosodium salt assay, while apoptosis was determined by terminal deoxynucleotidyl transferase-mediated dUTP nick end labeling stain. Immunofluorescent stains were performed using antibodies against phosphorylated Akt (pAkt) and cAMP response element binding protein (CREB) (pCREB), and ceramide. The mRNA expression and protein content of Bcl-2 were determined by reverse transcriptase-polymerase chain reaction and enzyme immunoassay, respectively. *In vivo* model of contrast-induced renal injury was induced in mice with unilateral renal occlusion. The cell injury induced by the nonionic radiocontrast medium ioversol was reversed by inhibiting *de novo* ceramide synthesis with fumonisin B<sub>1</sub> (FB<sub>1</sub>) and L-cycloserine, but not by suppressing sphingomyelin breakdown with D609. FB<sub>1</sub> reversed ioversol-induced decrease in the immunoreactivities of pAkt and pCREB, reduction in Bcl-2 expression and caspase-3 activation. Like ioversol, C2 ceramide and the Akt inhibitor Src homology-6 induced apoptosis by reducing pAkt and pCREB-like immunoreactivities, lowering Bcl-2 expression and enhancing caspase-3 activity. Indeed, various radiocontrast media, excluding iodixanol which showed the least nephrotoxicity, enhanced ceramide-like immunoreactivity. The role for *de novo* ceramide synthesis was also shown in the *in vivo* model of radiocontrast nephropathy. We demonstrated here for the first time that the enhancement of *de novo* ceramide synthesis contributes to radiocontrast nephropathy.

*Kidney International* (2006) **69**, 288–297. doi:10.1038/sj.ki.5000057

Correspondence: Y Itoh, Department of Pharmacy, Kyushu University Hospital, 3-1-1 Maidashi, Higashi-ku, Fukuoka 812-8582, Japan.  
E-mail: [yositou@st.hosp.kyushu-u.ac.jp](mailto:yositou@st.hosp.kyushu-u.ac.jp)

Received 2 June 2005; revised 19 July 2005; accepted 11 August 2005

KEYWORDS: radiocontrast medium; *de novo* ceramide synthesis; Akt; Bcl-2; apoptosis; renal tubular cells

Acute renal failure associated with iodinated radiocontrast media is still the major complication after radiographic examination, since it is associated with increased morbidity and mortality.<sup>1,2</sup> Unfortunately, there have been few effective medications for prevention of radiocontrast nephropathy. Although little is known about the etiology of radiocontrast nephropathy, the decrease in renal blood flow<sup>3</sup> and/or direct toxic action on renal tubular cells<sup>4</sup> are postulated to be implicated in the pathogenesis of radiocontrast nephropathy. Thus, a number of agents that improve renal vascular circulation, including endothelin antagonists, adenosine antagonists such as theophylline, atrial natriuretic peptide, dopamine agonists and calcium channel blockers, have been clinically investigated for the prevention of radiocontrast nephropathy, but most of them failed to succeed in preventing radiocontrast nephropathy in high-risk patients (for a review, see Cox and Tsikouris<sup>5</sup>). On the other hand, it has recently been reported that the antioxidant compound *N*-acetylcysteine<sup>6,7</sup> has a slight and not complete protective action against radiocontrast nephropathy, thereby suggesting that the radiocontrast nephropathy is associated with renal tubular injury due to the oxidative stress.

We have recently found that a variety of radiocontrast media cause cell injury in porcine renal tubular (LLC-PK<sub>1</sub>) cell line cells, as characterized by changes in the expression of B-cell lymphoma (Bcl)-2 family proteins such as Bcl-2 and Bax, activation of caspase-3 and nuclear fragmentation.<sup>8</sup> We also found that the radiocontrast medium inhibits the phosphorylation of Akt.<sup>9</sup> Since Akt is a serine/threonine kinase involved in cell survival and cell growth, the radiocontrast medium-induced apoptosis in renal tubular cells may be due to the inhibition of Akt phosphorylation. Indeed, the nonhydrolyzable cyclic AMP (cAMP) analog dibutyryl cAMP (DBcAMP) was found to attenuate renal tubular cell injury induced by the radiocontrast medium through activation of Akt, followed by phosphorylation of cAMP response element binding protein (CREB).<sup>10</sup> However, it is still uncertain how the radiocontrast medium inhibits phosphorylation of Akt in renal tubular cells.

It has been demonstrated that ceramide, a sphingolipid metabolite, decreases the level of phosphorylated Akt (pAkt)<sup>11,12</sup> and leads to apoptosis in a variety of cells.<sup>13,14</sup> Therefore, it seems likely that the contrast medium causes acute renal failure by elevating ceramide concentration in renal tubular cells. To ascertain this idea, we investigated the effects of several compounds that interfere with sphingolipid metabolism on renal tubular cell injury induced *in vitro* as well as *in vivo* by the radiocontrast medium. The effects of various nonionic radiocontrast media on the ceramide-like immunoreactivity were also examined in cultured renal tubular cells.

## RESULTS

### Effects of inhibitors of *de novo* ceramide synthesis and those of sphingomyelin breakdown on the loss of cell viability induced in porcine proximal tubular cells by ioversol

As shown in Figure 1, ioversol caused a significant decrease in cell viability, which was reversed by fumonisins B<sub>1</sub> (FB<sub>1</sub>), a specific inhibitor of ceramide synthase,<sup>15</sup> and L-cycloserine, an inhibitor of serine palmitoyltransferase,<sup>16</sup> but not by either D609, a xanthogenate compound that inhibits acidic sphingomyelinase activity through the inhibition of phosphatidylcholine-specific phospholipase C,<sup>17</sup> or the tricyclic antidepressant imipramine that inhibits sphingomyelinase activity.<sup>18</sup>

### Effect of FB<sub>1</sub> on ioversol-induced inhibition of phosphorylations of Akt and CREB

As shown in Figure 2a, the exposure of LLC-PK<sub>1</sub> cells to insulin-like growth factor-1 (IGF-1) markedly enhanced the

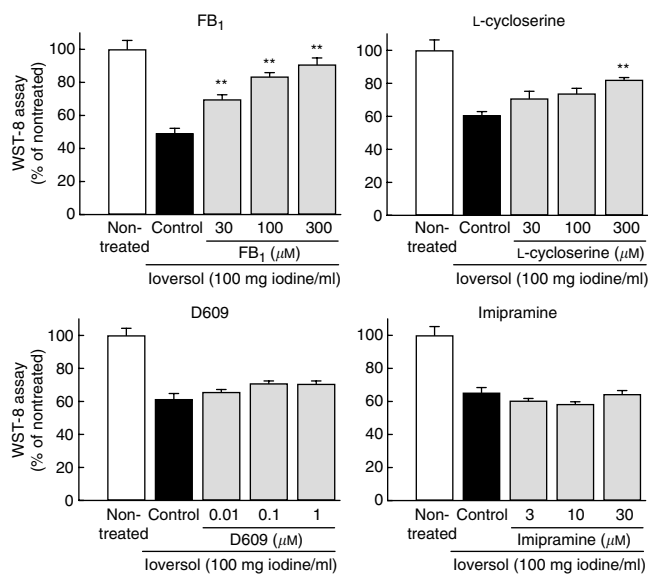


**Figure 1 | Effects of inhibitors of *de novo* ceramide synthesis and those of sphingomyelin breakdown on ioversol-induced loss of cell viability in LLC-PK<sub>1</sub> cells.** Cells were exposed to ioversol for 30 min, followed by incubation for 24 h in the absence of ioversol, and the viability was assessed by WST-8 assay. FB<sub>1</sub>, L-cycloserine, D609 and imipramine were added 30 min before ioversol and included throughout the experiment. Each column represents the mean ± s.e.m. of five experiments. \*\**P* < 0.01 vs control.

immunoreactivity for pAkt (Ser<sup>473</sup>), which was completely inhibited by Src homology (SH)-6, a specific Akt inhibitor that binds selectively to the pleckstrin homology domain of Akt to prevent the association of Akt with plasma membrane phosphatidylinositol-3-phosphate,<sup>19</sup> thereby suggesting that the immunoreactivity is derived from pAkt. Ioversol markedly inhibited the IGF-1-stimulated phosphorylation of Akt in a manner dependent on *de novo* ceramide synthesis. C2 ceramide also markedly inhibited the phosphorylation of Akt. On the other hand, protein level of pAkt as determined by the enzyme immunoassay was also reduced by ioversol, C2 ceramide and SH-6, in which the effect of ioversol was reversed by FB<sub>1</sub> (Figure 2b). Similar changes were observed for the phosphorylation of CREB and the level of phosphorylated CREB (pCREB).

### Effect of FB<sub>1</sub> on ioversol-induced depolarization of mitochondrial membranes and changes in expression of Bcl-2 family proteins

As shown in Figure 3a, fluorescent images for 5,5,6,6-tetrachloro-1,1,3,3-tetraethylbenzimidazolylcarbocyanine iodide (JC-1) were changed in color from red (J-aggregates) to green (monomers) after exposure to ioversol, suggesting that ioversol causes depolarization of mitochondrial membranes. FB<sub>1</sub> abolished, while C2 ceramide and SH-6 mimicked, the action of ioversol.

Since mitochondrial membrane potential is reported to be regulated by Bcl-2 family proteins such as Bcl-2 and Bax,<sup>20</sup> we investigated the changes in mRNA expression of and protein levels of Bcl-2 and Bax after exposure to ioversol in the absence or presence of FB<sub>1</sub>. As shown in Figure 3b and c, ioversol inhibited mRNA expression of Bcl-2 and decreased the level of Bcl-2 protein, while it enhanced mRNA expression of Bax and increased the level of Bax protein. These actions of ioversol were almost completely reversed by FB<sub>1</sub>. Similar changes in mRNA expressions and protein contents of these Bcl-2 family proteins were observed after exposure to C2 ceramide and SH-6.

### Effect of a caspase-3 inhibitor on apoptosis and loss of cell viability induced by ioversol, C2 ceramide, and SH-6 in LLC-PK<sub>1</sub> cells

As shown in Figure 4a, z-Asp(O-Me)-Glu(O-Me)-Val-Asp(O-Me) fluoromethyl ketone a specific caspase-3 inhibitor, reversed the appearance of terminal deoxynucleotidyl transferase-mediated dUTP nick end labeling (TUNEL)-positive cells induced by ioversol, C2 ceramide and SH-6. Moreover, the loss of cell viability induced by these agents was also reversed by z-Asp(O-Me)-Glu(O-Me)-Val-Asp(O-Me) fluoromethyl ketone (Figure 4b).

### Effects of ioversol, C2 ceramide, and SH-6 on caspase-3 activity in LLC-PK<sub>1</sub> cells

As shown in Figure 4c, the caspase-3 activity determined by the enzymatic degradation of caspase-3-specific substrate peptide was markedly enhanced by ioversol, C2 ceramide, and SH-6.

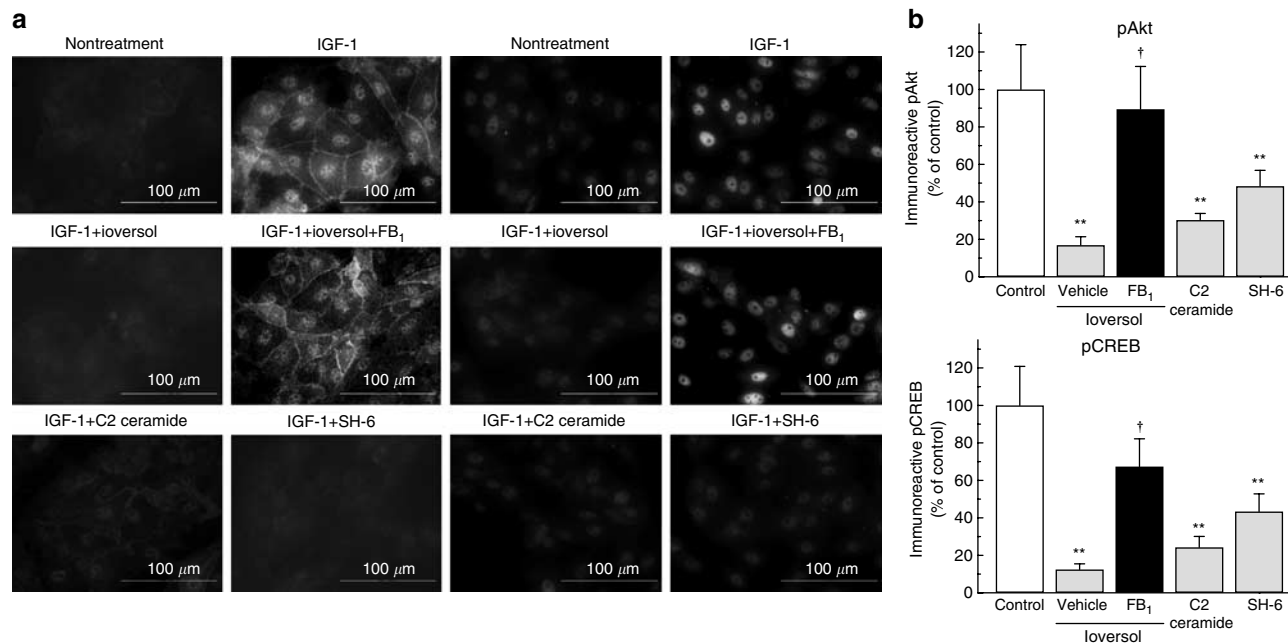


**Figure 2 | Involvement of ceramide in the decrease in phosphorylations of Akt and CREB (a) and basal levels of phosphorylated forms of Akt and CREB (b) induced in LLC-PK<sub>1</sub> cells by ioversol.** (a) Cells were incubated with IGF-1 in the absence or presence of ioversol, C2 ceramide or SH-6 for 30 min. FB<sub>1</sub> (300 nM) was included 30 min before ioversol. Cells were then fixed and immunofluorescent stained with antibodies raised against pAkt (Ser<sup>473</sup>) or pCREB (Ser<sup>133</sup>). (b) The basal levels of pAkt and pCREB were determined by enzyme immunoassay. Each column represents the mean ± s.e.m. of four or five experiments. \*\**P* < 0.01 vs control, †*P* < 0.05 vs vehicle.

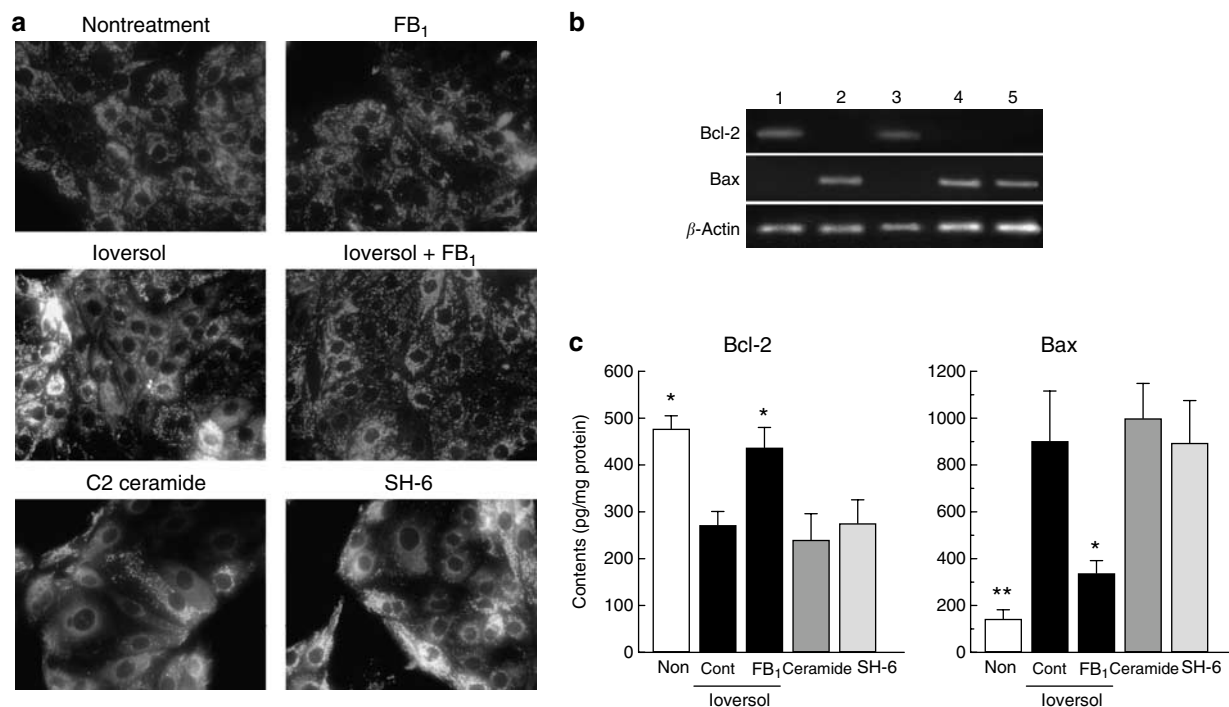


**Figure 3 | (a) Involvement of ceramide in the depolarization of mitochondrial membranes as assessed by JC-1 stain and (b) changes in mRNA expression and (c) protein levels of Bcl-2 and Bax induced in KKC-PK<sub>1</sub> cells by ioversol.** (a) Changes in fluorescent images were monitored after exposure to ioversol in the absence or presence of FB<sub>1</sub> (300 nM), C2 ceramide or SH-6. (b) The mRNA expressions for Bcl-2 and Bax were assessed by RT-PCR. Lane 1, nontreatment; lane 2, ioversol alone; lane 3, ioversol + FB<sub>1</sub>; lane 4, C2 ceramide; lane 5, SH-6. (c) The protein contents of Bcl-2 and Bax were determined by the enzyme immunoassay. Each column represents the mean ± s.e.m. of five experiments. \**P* < 0.05, \*\**P* < 0.01 vs control.

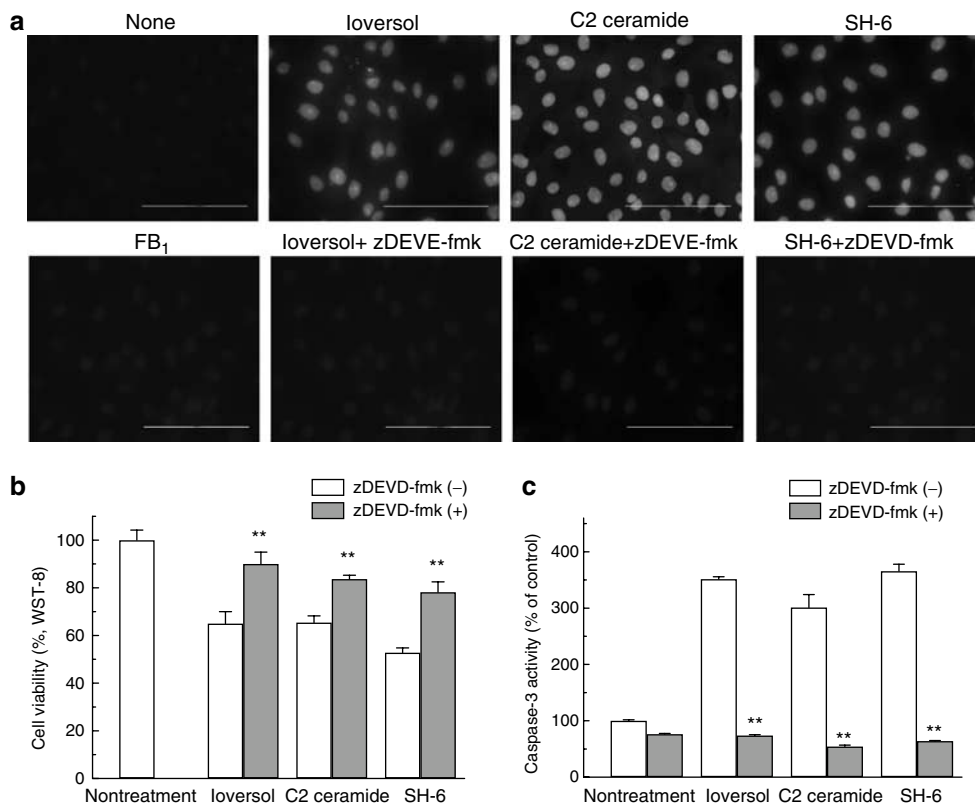


**Figure 4 | Effect of a caspase-3 inhibitor on (a) apoptosis, (b) loss of cell viability, and (c) enhancement of caspase-3 activity induced in LLC-PK<sub>1</sub> cells by ioversol, C2 ceramide and SH-6. (a)** Cells were exposed ioversol (100 mg iodine/ml) for 30 min, followed by incubation for 24 h in the absence of ioversol, or incubated with C2 ceramide or SH-6 for 24 h, then apoptosis was assessed by TUNEL stain. **(b)** Cell viability was measured by WST-8 assay. **(c)** Caspase-3 activity was determined by the enzymatic degradation of caspase-3-specific substrate peptide in the absence or presence of zDEVD-fmk. Each column represents the mean  $\pm$  s.e.m. of five experiments. \*\* $P < 0.01$  vs zDEVD-fmk (-).

#### Changes in ceramide-like immunoreactivity in LLC-PK<sub>1</sub> cells after exposure to ioversol in the absence or presence of FB<sub>1</sub> and D609

The exposure of LLC-PK<sub>1</sub> cells to ioversol for 30 min increased the ceramide-like immunoreactivity, as determined by immunofluorescent stain with anticeramide antibody, followed by flow-cytometric analysis (Figure 5a). The ioversol-induced increase in ceramide-like immunoreactivity was reversed by FB<sub>1</sub> (300 nM), but not by D609 (1  $\mu$ M).

#### Effects of a variety of radiocontrast media on ceramide-like immunoreactivity and cell viability

Like ioversol, several nonionic radiocontrast media, including iohexol, iomeprol, iopamidol, and iotrolan, enhanced the ceramide-like immunoreactivity (Figure 5b). Moreover, these contrast media reduced the cell viability determined by 2-(2-methoxy-4-nitrophenyl)-3-(4-nitrophenyl)-5-(2,4-disulfophenyl)-2H-tetrazolium monosodium salt (WST-8) assay, although the reduction in cell viability was slight (decrease by 10.5%) and not significant in iomeprol-exposed cells (Figure 5c). By contrast, iodixanol had no significant influence on ceramide-like immunoreactivity. The cell viability also did not change (decrease by 2.4%) after exposure to iodixanol.

#### Effect of FB<sub>1</sub> on renal injury and changes in cellular events induced by intravenous injection of ioversol in mice with unilateral renal occlusion

As we reported previously,<sup>9</sup> a single intravenous injection of ioversol-induced apoptosis in renal tubular cells (Figure 6a) and significant elevation of urinary activity of *N*-acetyl- $\beta$ -D-glucosaminidase (NAG), a specific marker of proximal renal tubular cell injury,<sup>21</sup> in mice with unilateral renal occlusion (Figure 6b). FB<sub>1</sub> (0.075 and 0.25 mg/kg) inhibited the apoptosis and enhancement of urinary NAG excretion induced by ioversol in a dose-dependent manner. Ioversol also lowered protein levels of pAkt (Figure 6c) and pCREB (Figure 6d) and enhanced caspase-3 activity (Figure 6e) in renal tissues. Interestingly, these cellular events induced by ioversol were all remarkably reversed by 0.25 mg/kg FB<sub>1</sub>. However, a high dose of FB<sub>1</sub> (2 mg/kg) was not effective in attenuating the ioversol-induced increase in urinary NAG excretion (NAG in U/g Cr:  $242.8 \pm 10.4$ , mean  $\pm$  s.e.m.,  $N = 4$ , for ioversol alone vs  $235.7 \pm 14.5$ ,  $N = 4$  for ioversol + FB<sub>1</sub> at 2 mg/kg).

#### DISCUSSION

We have previously shown that ioversol causes concentration- and time-dependent decreases in the viability of

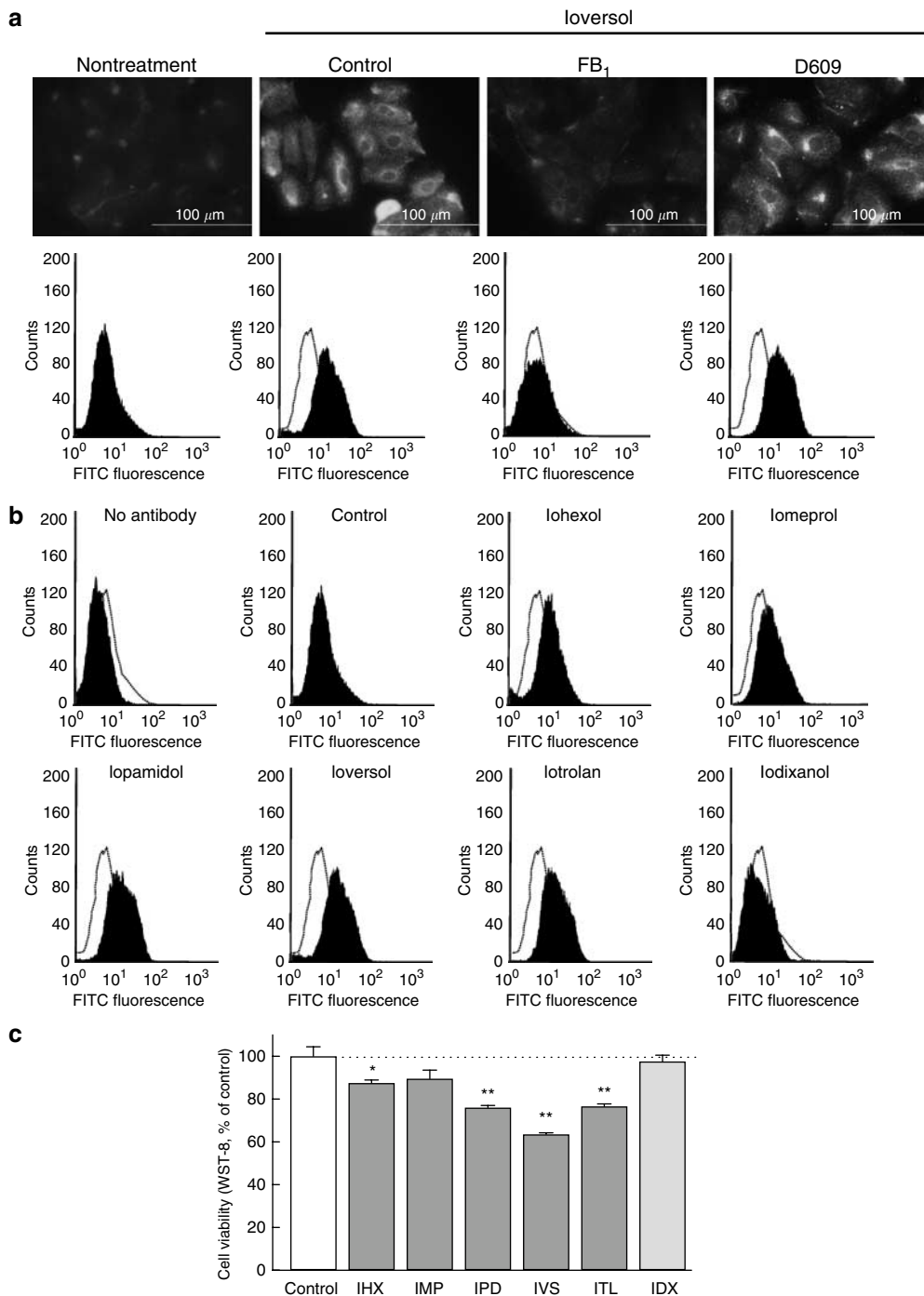


**Figure 5 | (a) Effects of FB<sub>1</sub> and D609 on ioversol-induced increase in ceramide-like immunoreactivity and (b) comparative effects of a variety of radiocontrast media on ceramide-like immunoreactivity and (c) cell viability in LLC-PK<sub>1</sub> cells. (a) Cells were exposed to ioversol for 30 min in the absence or presence of FB<sub>1</sub> (300 nM) or D609 (1 μM), and fluorescent images of ceramide-like immunoreactivity were monitored (upper) and analyzed by flow cytometry (lower). (b) Cells were exposed to various nonionic contrast media for 30 min and stained with ceramide antibody, then the immunoreactivity was analyzed by flow cytometry. (c) Cell viability was assessed by WST-8 assay 24 h after the transient exposure to radiocontrast media. Data were obtained from five experiments. \**P* < 0.05, \*\**P* < 0.01 vs control.**

LLC-PK<sub>1</sub> cells, in which significant injury is observed in as low as 25 mg iodine/ml of the contrast medium.<sup>8</sup> Moreover, the toxic effect of ioversol reaches maximum at 100 mg iodine/ml and the half-maximal reduction in the cell viability is observed at 24 h after exposure to 100 mg iodine/ml of the contrast medium. Thus, in the present study, we examined

the effects of compounds that interfere with sphingolipid metabolisms on the cell injury induced at 24 h by exposure to 100 mg iodine/ml of ioversol.

In the present study, the ioversol-induced injury of LLC-PK<sub>1</sub> cells was reversed concentration-dependently by the ceramide synthase inhibitor FB<sub>1</sub> and the serine palmitoyltransferase

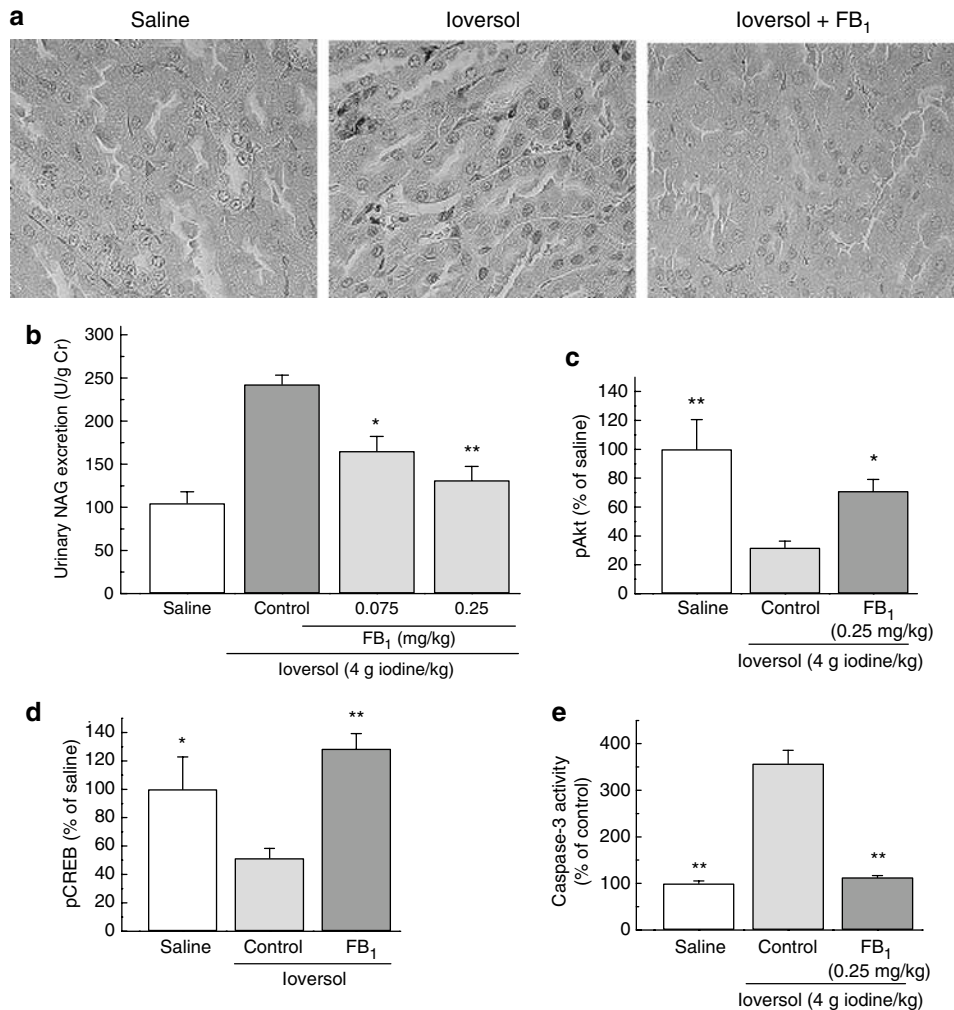


**Figure 6 | Effect of FB<sub>1</sub> on the (a) histological damage of renal tissues, (b) the enhancement of urinary excretion of NAG, (c) decrease in basal levels of pAkt, and (d) pCREB, and (e) the enhancement of caspase-3 activity induced in mice with unilateral renal ligation after intravenous injection of ioversol. (a)** Mice were injected with ioversol 7 days after unilateral renal ligation. FB<sub>1</sub> was administered subcutaneously 15 min before ioversol injection. Apoptosis was detected by TUNEL stain. **(b)** Urinary NAG activity was determined at 24 h after ioversol injection. Each column represents the mean  $\pm$  s.e.m. of five to six animals. **(c–e)** Right kidneys were dissected at 12 h after ioversol injection. FB<sub>1</sub> was administered subcutaneously at a dose of 0.25 mg/kg. The basal levels of pAkt and pCREB in renal tissues were determined by the enzyme immunoassay. Caspase-3 activity in the kidney medulla was assessed by enzymatic degradation of the specific substrate peptide. Each column represents the mean  $\pm$  s.e.m. of **(c, d)** four to six or **(e)** four experiments. \* $P < 0.05$ , \*\* $P < 0.01$  vs control.

inhibitor L-cycloserine, but not by inhibitors of sphingomyelin breakdown, such as D609 and imipramine. Therefore, it is suggested that ioversol causes renal tubular cell damage by enhancing *de novo* ceramide synthesis.

In our previous report, ioversol-induced injury of renal tubular cells is characterized by nuclear fragmentation, Annexin V-positive stain and the activation of caspase-9 and caspase-3, suggesting apoptosis.<sup>8,22</sup> Moreover, the apoptotic cell death is attributable to the mitochondrial stress due to changes in Bcl-2 family proteins such as Bcl-2 and Bax.<sup>8</sup> It has been demonstrated that the relative increase in the expression of Bax over Bcl-2 leads to the depolarization of mitochondrial membranes and stimulates the release of cytochrome *c*, which, in turn, activates caspase-9 through the action of the adaptor molecule apoptotic protease-activating

factor-1.<sup>23</sup> Consistent with our previous data, in the present study, ioversol caused the depolarization of mitochondrial membranes as assessed by JC-1 stain, activation of caspase-3 and ultimately led to caspase-3-dependent apoptosis determined by TUNEL stain.

We also found previously that DBcAMP protects renal tubular cells against ioversol-induced apoptosis through phosphorylation of Akt and CREB and subsequent enhancement of Bcl-2 expression.<sup>8–10,22</sup> Interestingly, ioversol was found to inhibit phosphorylation of Akt at Ser<sup>473</sup> and phosphorylation of CREB at Ser<sup>133</sup>.<sup>10</sup>

It has been demonstrated that Akt plays an important role in the cell survival since inhibition of propidium iodide 3-kinase/Akt stimulates caspase activity and leads to apoptosis in a variety of cells.<sup>24–26</sup> Moreover, phosphorylation

of Akt is reported to upregulate the expression of Bcl-2 through phosphorylation of CREB.<sup>27,28</sup>

In the present study, IGF-1 enhanced not only the pAkt-like immunoreactivity but also the pCREB-like immunoreactivity in LLC-PK<sub>1</sub> cells. In addition, IGF-1-mediated phosphorylation of CREB was diminished by SH-6, thereby suggesting that the phosphorylation of CREB is mediated through the activation of Akt in these cells.

It has been demonstrated that the membrane sphingolipid ceramide decreases the level of phosphorylated form of Akt by facilitating the dephosphorylation of Akt at Ser<sup>473</sup> through the activation of protein phosphatase 2A<sup>11</sup> and/or by inhibiting the association of pleckstrin homology domain of Akt with membrane proximal intraglomerular pressure 3 through the activation of protein kinase C<sub>ε</sub>.<sup>29</sup>

In the present study, it was noteworthy that the inhibition by ioversol of IGF-1-induced phosphorylation of Akt was abolished by FB<sub>1</sub>. Moreover, C2 ceramide showed a marked inhibition on IGF-1-induced phosphorylation of Akt. Therefore, it is highly probable that the inhibition of the phosphorylation of Akt induced by ioversol is attributable to the enhancement of *de novo* ceramide synthesis.

FB<sub>1</sub> was also effective in suppressing ioversol-induced inhibition of IGF-1-stimulated phosphorylation of CREB, while C2 ceramide and SH-6 markedly reduced the IGF-1-stimulated phosphorylation of CREB. Moreover, down-regulation of Bcl-2 and upregulation of Bax induced by ioversol were reversed by FB<sub>1</sub>, while C2 ceramide and SH-6 caused similar changes in the expression of these Bcl-2 family proteins to ioversol. Taken together, it is suggested that ioversol stimulates *de novo* ceramide synthesis, which leads to apoptosis by inhibiting the phosphorylation of Akt and CREB and subsequent reduction of Bcl-2 expression and activation of caspase-3.

It has been demonstrated that a number of apoptotic stimuli such as reactive oxygen species<sup>30</sup> and tumor necrosis factor (TNF)- $\alpha$ <sup>31</sup> increase the ceramide content by facilitating sphingomyelin breakdown, but not through the activation of the *de novo* synthesis pathway. In the present study, both the enhancement of ceramide-like immunoreactivity and cell injury induced by ioversol were not affected by inhibiting sphingomyelin breakdown with D609 or imipramine. Therefore, it is unlikely that sphingomyelin breakdown plays a role in renal tubular injury induced by the radiocontrast medium. On the other hand, a role for reactive oxygen species in the pathogenesis of radiocontrast nephropathy has been shown by several clinical findings indicating that the antioxidant *N*-acetylcysteine is effective for the prevention of radiocontrast nephropathy in patients with pre-existing renal insufficiency.<sup>6,7</sup> We do not know whether *N*-acetylcysteine is effective for prevention of apoptosis of LLC-PK<sub>1</sub> cells induced by radiocontrast media. However, Hizoh and Haller<sup>32</sup> have shown in cultured Madin Darby Canine Kidney cells that *N*-acetylcysteine has no protective action against the nuclear damage induced by the ionic contrast medium amidotrizoate. At present, it is uncertain whether reactive oxygen species

contribute to the increase in ceramide content or apoptosis induced by radiocontrast media.

In the present study, like ioversol, a variety of iodinated radiocontrast media enhanced ceramide-like immunoreactivity in renal tubular cells. However, iomeprol caused only a slight increase in the ceramide-like immunoreactivity, while iodixanol had no effect on the immunoreactivity. It was noteworthy that the increase in the ceramide-like immunoreactivity was closely associated with the loss of cell viability.

It has been demonstrated by the clinical studies that the risk of radiocontrast nephropathy is much lower in iodixanol than in other low osmolar media.<sup>33</sup> It is generally considered that high osmolality is the major causative factor of radiocontrast nephropathy.<sup>34</sup> However, in the present study, another iso-osmolar contrast medium iotrolan, whose osmolality is equivalent to that of iodixanol, produced a marked decrease in cell viability as well as an enhancement of ceramide-like immunoreactivity. Taken together, it is suggested that the enhancement of *de novo* ceramide synthesis is the common cellular mechanism underlying renal tubular injury induced by a variety of iodinated radiocontrast media.

Finally, we investigated the effect of FB<sub>1</sub> on the *in vivo* renal injury induced by ioversol in mice with unilateral renal occlusion. Deray *et al.*<sup>35</sup> reported that the radiocontrast medium enhances urinary excretion of NAG in rats with renal artery occlusion, but not in intact animals. Generally consistent with their data, in the present study, ioversol enhanced urinary NAG excretion in mice with unilateral renal occlusion. Moreover, a number of TUNEL-positive cells appeared in the tubular region. Therefore, the present model of radiocontrast-induced renal injury is due, at least in part, to renal tubular cell apoptosis. Systemic injection of FB<sub>1</sub> (0.075 and 0.25 mg/kg) prevented the apoptosis and urinary NAG excretion, suggesting an involvement of *de novo* ceramide synthesis *in vivo*. Moreover, as observed in cultured renal tubular cells, ioversol injection caused a marked reduction in the protein levels of pAkt and pCREB and the activation of caspase-3, all of which were remarkably reversed by FB<sub>1</sub> (0.25 mg/kg). However, a high dose of FB<sub>1</sub> (2 mg/kg) was not effective in attenuating the ioversol-induced increase in urinary NAG excretion. This may be due to the toxic action of FB<sub>1</sub>. It has been reported that repeated injection of FB<sub>1</sub> (at doses higher than 0.25 mg/kg for 5 days) induces apoptosis in the kidney of mice.<sup>36</sup> FB<sub>1</sub> is also reported to cause apoptosis in LLC-PK<sub>1</sub> cells, in which accumulation of sphinganine due to the inhibition of ceramide synthase inhibition is involved.<sup>37</sup> However, the minimal concentration of FB<sub>1</sub> for eliciting cell injury is reported to be 35  $\mu$ M,<sup>38</sup> a concentration that is much higher than the IC<sub>50</sub> value (0.1  $\mu$ M) for inhibiting ceramide synthase activity in rat liver microsomes<sup>15</sup> and those used in the present study. Seefelder *et al.*<sup>39</sup> have shown the lack of involvement of ceramide synthase inhibition in FB<sub>1</sub>-induced apoptosis, since other fumonisin analogs that inhibit ceramide synthase activity have no toxic action on renal tubular cells. It has been

reported that TNF- $\alpha$  contributes to the *in vivo* and *in vitro* toxic actions of FB<sub>1</sub>.<sup>40,41</sup>

In conclusion, we demonstrated here for the first time that radiocontrast media enhance *de novo* ceramide synthesis and induce renal tubular cell apoptosis through the inhibition of Akt phosphorylation, followed by CREB phosphorylation. Moreover, the ceramide synthase inhibitor was fully effective in attenuating renal tubular cell injury induced *in vitro* as well as *in vivo* by the radiocontrast medium. Therefore, the inhibition of *de novo* sphingolipid synthesis pathway may become a novel and potentially useful approach to the prophylaxis of radiocontrast nephropathy.

Moreover, our present findings may help to develop the novel radiocontrast media devoid of nephrotoxicity by screening the compounds that have no influence on sphingolipid metabolism.

## MATERIALS AND METHODS

### Materials

The iodinated radiographic contrast media used in the present study were as follows: iohexol (Omnipaque 300<sup>®</sup>, 300 mg iodine/ml, Daiichi Pharmaceutical, Tokyo, Japan), iomeprol (Iomeron 400<sup>®</sup>, 400 mg iodine/ml, Eisai, Tokyo, Japan), iopamidol (Iopamiron 300<sup>®</sup>, 300 mg iodine/ml, Schering AG, Berlin, Germany), ioversol (Optiray 350<sup>®</sup>, 350 mg iodine/ml, Ymanouchi Pharmaceutical, Tokyo, Japan), iotrolan (Isovist 300<sup>®</sup>, 300 mg iodine/ml, Schering AG, Berlin, Germany) and iodixanol (Visipaque 320<sup>®</sup>, 320 mg iodine/ml, Daiichi Pharmaceutical, Tokyo, Japan). The concentration of radiographic contrast media used in the present *in vitro* study was 100 mg iodine/ml, while the dose of ioversol used *in vivo* study was 4 g iodine/kg. The following chemicals and reagents were obtained from commercial sources: the Akt inhibitor D-2,3-dideoxy-myoinositol 1-((R)-2-methoxy-3-(octadecyloxy)propyl hydrogen phosphate) (SH-6: 1  $\mu$ M) and the fluorescence-labeled peptide substrate specific for caspase-3 Ac-DEVD-7-amino-4-methylcoumarin (AMC) (10  $\mu$ M: Alexis Biochemicals, San Diego, CA), IGF-1 (100 ng/ml) and the serine palmitoyltransferase inhibitor L-cycloserine (30–300  $\mu$ M: Sigma, St Louis, MO, USA), the ceramide synthase inhibitor FB<sub>1</sub> (30–300 nM or 0.075–0.25 mg/kg), the inhibitors of sphingomyelin breakdown, such as imipramine (3–30  $\mu$ M) and potassium tricyclo(5.2.1.0<sup>2,6</sup>)decan-8-yl dithiocarbonate (D609: 0.01–1  $\mu$ M) and the fluorescent indicator of mitochondrial membrane potential JC-1 (10 ng/ml) (Wako Pure Chemical, Osaka, Japan), and C2 ceramide (3  $\mu$ M) (Cayman Chemical, Ann Arbor, MI, USA).

### Cell culture

LLC-PK<sub>1</sub> cells (Lily Laboratory Culture-Porcine Kidney) were obtained from the American Type Culture Collection (Rockville, MD, USA), were grown in a 75-cm<sup>2</sup> flask (Corning incorporated, Corning, NY, USA) and maintained in Medium 199 (ICN Biomedicals, Inc., Aurora, OH, USA) supplemented with 10% fetal bovine serum (JRH Bioscience, Inc., Lenexa, KS, USA) and 60  $\mu$ g/ml penicillin (Sigma) in an atmosphere of 5% CO<sub>2</sub> in air at 37°C. For the experiment, cells were seeded on 24-well plates (Falcon<sup>®</sup>, Becton Dickinson Co., Ltd, Franklin Lakes, NJ, USA) at a density of 1.0  $\times$  10<sup>4</sup> cells/cm<sup>2</sup>. and cultured at 37°C for 24 h.

### Cell injury

The cell injury was induced by exposure (30 min) to radiocontrast media, followed by further incubation for 24 h in normal medium,

or by incubating with C2 ceramide or SH-6 for 24 h. Then, the cell viability was estimated from the mitochondrial activity to reduce WST-8 to the water-soluble formazan, as described previously.<sup>8</sup> Briefly, cells were incubated at 37°C for 90 min in 210  $\mu$ l of serum-free medium containing 10  $\mu$ l of WST-8 assay solution (Cell Counting Kit-8, Dojindo Laboratory, Kumamoto, Japan). Aliquots of the incubation medium were transferred to 96-well microplates, and the absorbance was measured at 620 nm with the reference wavelength of 450 nm using a microplate reader (Immuno Mini NJ-2300, Inter Med, Tokyo, Japan). Apoptosis was assessed by TUNEL, as described previously.<sup>42</sup> Briefly, after exposure to various stimuli, cells were washed with phosphate-buffered saline (PBS) and fixed for 30 min at room temperature with 4% (w/v) paraformaldehyde in PBS. Then, the cells were permeabilized with 0.1% Triton X-100 in 0.1% sodium citrate solution. TUNEL stain was carried out using a commercial apoptosis assay kit (Cell Death Detection kit, Roche Applied Science, Tokyo, Japan), according to the manufacturer's instructions. The stained cells were visualized with a fluorescence microscope (BX51, Olympus, Tokyo, Japan) and a cooled charge-coupled device (CCD) camera (DP70, Olympus).

### Assay for caspase-3 activity

The activity of caspase-3 was determined by the degradation of the substrate peptide conjugated with a fluorescent probe AMC, as described previously.<sup>8</sup> The reaction was started by incubating enzyme extracts with the caspase substrate Ac-zDEVD-AMC (10  $\mu$ M) for 10 min in the absence or presence of 10  $\mu$ M zDEVD-fmk. The concentration of AMC liberated into the supernatant was determined fluorometrically at an excitation wavelength of 380 nm and an emission wavelength of 460 nm.

### Reverse transcription-polymerase chain reaction for Bcl-2 and Bax

The mRNAs for Bcl-2 and Bax were measured by reverse transcriptase-polymerase chain reaction (RT-PCR), as described previously.<sup>8</sup> The sequences of PCR primers were as follows: 5'-AGCGTCAACGGGAGATGTC-3' (sense) and 5'-GTGATGCAAGCTCCACCAG-3' (antisense) for Bcl-2, and 5'-CAGCTCTGAGCAGATCATGAAGACA-3' (sense) and 5'-GCCCATCTTCTTCCAGATGGTGAGC-3' (antisense) for Bax. Amplification of cDNA provided from murine renal tissues was carried out for 30 cycles (denaturation at 94°C for 45 s, annealing at 53°C for 45 s and elongation at 72°C for 90 s), followed by additional polymerization at 72°C for 7 min, using Apoptosis PCR Bax/Bcl-2 Multiplex Primer Sets (Sigma), according to the manufacturer's instruction. The PCR products were subjected to electrophoresis on 2% agarose gel, and visualized by ethidium bromide stain under ultraviolet irradiation.

### Measurement of Bcl-2 and Bax proteins

The protein contents of Bcl-2 and Bax were determined by the enzyme immunoassay, as described previously,<sup>42</sup> using the respective enzyme immunoassay kit (Oncogene Research Products, San Diego, CA, USA).

### Mitochondrial membrane potential as measured by JC-1 staining

Changes in mitochondrial membrane potentials were assessed by using JC-1 according to the method of Reers *et al.*<sup>43</sup> Briefly, cells were seeded on eight-chamber plastic slides at 2  $\times$  10<sup>4</sup> cells/cm<sup>2</sup> and incubated for 24 h, then exposed to various test compounds. At 12 h after the exposure, the culture medium was replaced by the medium



containing JC-1 and incubated for 15 min. Fluorescence images were observed using a fluorescence microscope and a cooled CCD camera (Olympus) at the excitation wavelength of 490 nm.

#### Immunofluorescent stain for pAkt and CREB (pCREB)

Immunofluorescent stains for pAkt and pCREB were carried out according to the method of Gupta *et al.*<sup>44</sup> and Ingfield *et al.*,<sup>45</sup> respectively. Briefly, cells were cultured on eight-chamber plastic slides and incubated for 24 h. After washing with PBS, cells were incubated with IGF-1 for 20 min in the absence or presence of test compounds. The chamber slides were rinsed with ice-cold PBS and fixed with 10% (w/v) ice-cold trichloroacetic acid for 30 min. The specific rabbit antibody raised against porcine pAkt (Ser<sup>473</sup>) (Cell Signaling Technology, Beverly, MA, USA) or rat antibody raised against porcine pCREB (Ser<sup>133</sup>) (Affinity Bioreagents, Golden, CO, USA) was diluted (1:50) with PBS containing 5% (w/v) non-fat dried milk and 0.1% Triton X-100. Cells were incubated with the diluted antibodies overnight in a humidified chamber at 4°C, then further incubated at room temperature for 2 h with fluorescein isothiocyanate (FITC)-labeled goat anti-rabbit immunoglobulin G (IgG) or anti-rat IgG (1:50 dilution with PBS) (The Jackson Laboratory, Bar Harbor, ME, USA). The fluorescence images were visualized using a fluorescent microscopy (BX51, Olympus, Tokyo, Japan).

#### Determination of pAkt- and pCREB-like immunoreactivities

The basal level of pAkt- or pCREB-like immunoreactivity was determined by the respective enzyme immunoassay (BioSource International, Camarillo, CA, USA). Briefly, cells were seeded in a 25-cm<sup>2</sup> flask, and incubated for 48 h, then exposed to ioversol for 30 min in the absence or presence of FB<sub>1</sub> (300 nM), followed by further incubation for 3 h, or otherwise cells were incubated with C2 ceramide or SH-6 for 3 h. In the *in vivo* experiment, kidneys were dissected 12 h after ioversol injection, and homogenized with 0.5 ml lysis buffer, then subjected to the enzyme immunoassay for pAkt or pCREB.

#### Immunofluorescent analysis for ceramide-like immunoreactivity

Cells were exposed to various radiocontrast media, then fixed with 3% (w/v) paraformaldehyde in PBS for 30 min at 4°C, and permeabilized with 0.1% Triton X-100. Subsequently, cells were incubated with anti-ceramide antibody (Alexis) diluted 1:50 with PBS containing 5% (w/v) nonfat dried milk for 1 h at room temperature. After washing with PBS, cells were incubated for 1 h at room temperature with FITC-labeled secondary antibody (Jackson Laboratory) diluted (1:100) with PBS containing 5% (w/v) nonfat dried milk. Fluorescent images were monitored by flow cytometry (Becton Dickinson).

#### *In vivo* model of radiocontrast-induced renal injury

The experimental procedure was approved by the Institutional Committee for the Care and Use of Laboratory Animals at the Kyushu University Hospital. The renal injury was induced in mice by a single intravenous injection of ioversol, as described previously.<sup>10</sup> Briefly, male ddY mice (Kyudo Co., Saga, Japan) weighing 30–35 g were anesthetized with pentobarbital-Na (50 mg/kg) and subjected to unilateral ligation of the left anterior renal pedicle, including renal artery, renal vein and ureter, or subjected to sham operation in which the incision of abdominal skin was made but the kidney was not ligated. At 7 days after the surgical procedure, mice were divided into two groups to perform two sets of

independent experiments, including the assessment of renal injury by measuring urinary NAG activity and histological observations, and the determination of cellular signals such as caspase-3 activity and phosphorylations of Akt and CREB. In both experiments, kidney-occluded mice were divided into three groups and injected subcutaneously with saline (control group), 0.075 mg/kg FB<sub>1</sub> or 0.25 mg/kg FB<sub>1</sub>, then injected intravenously with ioversol 15 min later. FB<sub>1</sub> was dissolved in saline. Sham-operated mice were injected intravenously with saline alone via the tail vein. In the experiment for assessing renal injury, the activity of NAG in urine was determined at 24 h by the enzymatic degradation of the substrate sodium cresol sulfonaphthaleinyl NAG using the commercial assay kit. Then, the right kidney was dissected and fixed in 20% formalin, dehydrated in graded concentrations of ethanol and embedded in paraffin. The kidney block was cut into 2- $\mu$ m sections and subjected to TUNEL stain. In another set of experiments where the intracellular signals were determined, the right kidney was dissected under deep anesthesia at 12 h after ioversol injection. The protein contents of pAkt and pCREB were determined by enzyme immunoassay. The activity of caspase-3 in renal tissues were also measured as described above.

#### Statistical analyses

Data are expressed as the mean  $\pm$  s.e.m. and statistically analyzed by one-way analysis of variance, followed by Dunnett's test for multiple comparisons or by two-tailed Student's *t*-test for comparison between two groups, or by the Kruskal–Wallis test combined with a Steel-type multiple comparison tests for nonparametric analysis.

#### ACKNOWLEDGMENTS

This research was supported in part by Grant-in-Aid for Scientific Research (C17590471) from the Ministry of Education, Science, Sport and Culture, Japan.

#### REFERENCES

1. Gruberg L, Mintz GS, Mehran R *et al.* Prognostic implications of further renal function deterioration within 48 h of interventional coronary procedures in patients with pre-existent chronic renal insufficiency. *J Am Coll Cardiol* 2000; **36**: 1542–1548.
2. Dargas G, Iakovou I, Nikolsky E *et al.* Contrast-induced nephropathy after percutaneous coronary interventions in relation to chronic kidney disease and hemodynamic variables. *Am J Cardiol* 2005; **95**: 13–19.
3. Liss P, Nygren A, Erikson U, Ulfendahl HR. Injection of low and iso-osmolar contrast medium decreases oxygen tension in the renal medulla. *Kidney Int* 1998; **53**: 698–702.
4. Zager RA, Johnson AC, Hanson SY. Radiographic contrast media-induced tubular injury: evaluation of oxidant stress and plasma membrane integrity. *Kidney Int* 2003; **64**: 128–139.
5. Cox CD, Tsikouris JP. Preventing contrast nephropathy: what is the best strategy? A review of the literature. *J Clin Pharmacol* 2004; **44**: 327–337.
6. Tepel M, van der Giet M, Schwarzfeld C *et al.* Prevention of radiographic contrast medium-induced reductions in renal function by acetylcysteine. *N Engl J Med* 2000; **343**: 180–184.
7. Pannu N, Manns B, Lee H, Tonelli M. Systematic review of the impact of N-acetylcysteine on contrast nephropathy. *Kidney Int* 2004; **65**: 1366–1374.
8. Yano T, Itoh Y, Sendo T *et al.* Cyclic AMP reverses radiocontrast media-induced apoptosis in LLC-PK<sub>1</sub> cells by activating A kinase/PI3 kinase. *Kidney Int* 2003; **64**: 2052–2063.
9. Yano T, Itoh Y, Kubota T *et al.* A prostacyclin analog beraprost sodium attenuates radiocontrast media-induced LLC-PK<sub>1</sub> cells injury. *Kidney Int* 2004; **65**: 1654–1663.
10. Yano T, Itoh Y, Kubota T *et al.* A prostacyclin analog prevents radiocontrast nephropathy via phosphorylation of cyclic AMP response element binding protein. *Am J Pathol* 2005; **166**: 1333–1342.

11. Schubert KM, Scheid MP, Duronio V. Ceramide inhibits protein kinase B/Akt by promoting dephosphorylation of serine<sup>473</sup>. *J Biol Chem* 2000; **275**: 13330–13335.
12. Stoica BA, Movsesyan VA, Lea IV PM, Faden AI. Ceramide-induced neuronal apoptosis is associated with dephosphorylation of Akt, BAD, FKHR, GSK-3 $\beta$ , and induction of the mitochondrial-dependent intrinsic caspase pathway. *Mol Cell Neurosci* 2003; **22**: 365–382.
13. Iwata M, Herrington J, Zager RA. Sphingosine: a mediator of acute renal tubular injury and subsequent cytoresistance. *Proc Natl Acad Sci USA* 1995; **92**: 8970–8974.
14. Ueda N, Kaushal GP, Hong X, Shah SV. Role of enhanced ceramide generation in DNA damage and cell death in chemical hypoxic injury to LLC-PK<sub>1</sub> cells. *Kidney Int* 1998; **54**: 399–406.
15. Wang E, Norred WP, Bacon CW et al. Inhibition of sphingolipid biosynthesis by fumonisins. Implications for diseases associated with *Fusarium moniliforme*. *J Biol Chem* 1991; **266**: 14486–14490.
16. Holleran WM, Williams ML, Gao WN, Elias PM. Serine-palmitoyl transferase activity in cultured human keratinocytes. *J Lipid Res* 1990; **31**: 1655–1661.
17. Luberto C, Hannun YA. Sphingomyelin synthase, a potential regulator of intracellular levels of ceramide and diacylglycerol during SV40 transformation. Does sphingomyelin synthase account for the putative phosphatidylcholine-specific phospholipase C? *J Biol Chem* 1998; **273**: 14550–14559.
18. Albouz S, Vanier MT, Hauw JJ et al. Effect of tricyclic antidepressants on sphingomyelinase and other sphingolipid hydrolases in C6 cultured glioma cells. *Neurosci Lett* 1983; **36**: 311–315.
19. Meuillet EJ, Mahadevan D, Vankayalapati H et al. Specific inhibition of the Akt1 pleckstrin homology domain by D-3-deoxy-phosphatidyl-myo-inositol analogues. *Mol Cancer Ther* 2003; **2**: 389–399.
20. Kroemer G. The proto-oncogene Bcl-2 and its role in regulating apoptosis. *Nat Med* 1997; **3**: 614–620.
21. Bourbouze R, Baumann FC, Bonvalet JP, Farman N. Distribution of N-acetyl- $\beta$ -D-glucosaminidase isoenzymes along the rabbit nephron. *Kidney Int* 1984; **25**: 636–642.
22. Itoh Y, Yano T, Sendo T, Oishi R. Critical review: clinical and experimental evidence for prevention of acute renal failure induced by radiographic contrast media. *J Pharmacol Sci* 2005; **97**: 473–488.
23. Robertson JD, Orrenius S. Role of mitochondria in toxic cell death. *Toxicology* 2002; **181–182**: 491–496.
24. Kandel ES, Hay N. The regulation and activities of the multifunctional serine/threonine kinase Akt/PKB. *Exp Cell Res* 1999; **253**: 210–229.
25. Goswami R, Dawson SA, Dawson G. Multiple polyphosphoinositide pathways regulate apoptotic signalling in a dorsal root ganglion derived cell line. *J Neurosci Res* 2000; **59**: 136–144.
26. Datta SR, Brunet A, Greenberg ME. Cellular survival: a play in three Acts. *Genes Dev* 1999; **13**: 2905–2927.
27. Pugazhenthii S, Nesterova A, Sable C et al. Akt/protein kinase B up-regulates Bcl-2 expression through cAMP-response element-binding protein. *J Biol Chem* 2000; **275**: 10761–10766.
28. Pugazhenthii S, Miller E, Sable C et al. Insulin-like growth factor-I induces bcl-2 promoter through the transcription factor cAMP-response element-binding protein. *J Biol Chem* 1999; **274**: 27529–27535.
29. Powell DJ, Hajdich E, Kular G, Hundal HS. Ceramide disables 3-phosphoinositide binding to the pleckstrin homology domain of protein kinase B (PKB)/Akt by a PKCzeta-dependent mechanism. *Mol Cell Biol* 2003; **23**: 7794–7808.
30. Martin D, Salinas M, Fujita N et al. Ceramide and reactive oxygen species generated by H<sub>2</sub>O<sub>2</sub> induce caspase-3-independent degradation of Akt/protein kinase B. *J Biol Chem* 2002; **277**: 42943–44952.
31. Liu B, Andrieu-Abadie N, Levade T et al. Glutathione regulation of neutral sphingomyelinase in tumor necrosis factor-alpha-induced cell death. *J Biol Chem* 1998; **273**: 11313–11320.
32. Hizoh I, Haller C. Radiocontrast-induced renal tubular cell apoptosis: hypertonic versus oxidative stress. *Invest Radiol* 2002; **37**: 428–434.
33. Aspelin P, Aubry P, Fransson SG et al. Nephrotoxicity in high-risk patients study of iso-osmolar and low-osmolar non-ionic contrast media study investigators. Nephrotoxic effects in high-risk patients undergoing angiography. *N Engl J Med* 2003; **348**: 491–499.
34. Barrett BJ, Carlisle EJ. Metaanalysis of the relative nephrotoxicity of high- and low-osmolality iodinated contrast media. *Radiology* 1993; **188**: 171–178.
35. Deray G, Dubois M, Martinez F et al. Renal effects of radiocontrast agents in rats: a new model of acute renal failure. *Am J Nephrol* 1990; **10**: 507–513.
36. Sharma RP, Dugyala RR, Voss KA. Demonstration of *in-situ* apoptosis in mouse liver and kidney after short-term repeated exposure to fumonisin B<sub>1</sub>. *J Comp Pathol* 1997; **117**: 371–381.
37. Kim MS, Lee DY, Wang T, Schroeder JJ. Fumonisin B<sub>1</sub> induces apoptosis in LLC-PK<sub>1</sub> renal epithelial cells via a sphinganine- and calmodulin-dependent pathway. *Toxicol Appl Pharmacol* 2001; **176**: 118–126.
38. Yoo HS, Norred WP, Wang E et al. Fumonisin inhibition of *de novo* sphingolipid biosynthesis and cytotoxicity are correlated in LLC-PK<sub>1</sub> cells. *Toxicol Appl Pharmacol* 1993; **114**: 9–15.
39. Seefelder W, Humpf HU, Schwerdt G et al. Induction of apoptosis in cultured human proximal tubule cells by fumonisins and fumonisin metabolites. *Toxicol Appl Pharmacol* 2003; **192**: 146–153.
40. Dugyala RR, Sharma RP, Tsunoda M, Riley RT. Tumor necrosis factor-alpha as a contributor in fumonisin B<sub>1</sub> toxicity. *J Pharmacol Exp Ther* 1998; **285**: 317–324.
41. Voss KA, Howard PC, Riley RT et al. Carcinogenicity and mechanism of action of fumonisin B<sub>1</sub>: a mycotoxin produced by *Fusarium moniliforme* (*F. verticillioides*). *Cancer Detect Prev* 2002; **26**: 1–9.
42. Kubota T, Fujisaki K, Itoh Y et al. Apoptotic injury in cultured human hepatocytes induced by HMG-CoA reductase inhibitors. *Biochem Pharmacol* 2004; **67**: 2175–2186.
43. Reers M, Smith TW, Chen LB. J-aggregate formation of a carbocyanine as a quantitative fluorescent indicator of membrane potential. *Biochemistry* 1991; **30**: 4480–4486.
44. Gupta AK, McKenna WG, Weber CN et al. Local recurrence in head and neck cancer: relationship to radiation resistance and signal transduction. *Clin Cancer Res* 2002; **8**: 885–889.
45. Inglefield JR, Mundy WR, Meacham CA, Shafer TJ. Identification of calcium-dependent and -independent signaling pathways involved in polychlorinated biphenyl-induced cyclic AMP-responsive element-binding protein phosphorylation in developing cortical neurons. *Neuroscience* 2002; **115**: 559–573.